Hindawi Publishing Corporation
International Journal of Distributed Sensor Networks
Volume 2012, Article ID 861704, 11 pages
doi:10.1155/2012/861704

Research Article

Energy-Model-Based Optimal Communication Systems Design for Wireless Sensor Networks

Ye Li, Dengyu Qiao, Zhao Xu, Da Xu, Fen Miao, and Yuwei Zhang

The Key Lab for Health Informatics of Chinese Academy of Sciences, Shenzhen Institutes of Advanced Technology, Chinese Academy of Sciences, Shenzhen 518055, China

Correspondence should be addressed to Ye Li, ye.li@siat.ac.cn

Received 29 June 2012; Revised 22 September 2012; Accepted 3 October 2012

Academic Editor: George P. Efthymoglou

As is widely used in our daily life, wireless sensor network (WSN) is considered as one of the most important technologies of the new century. Although, the sensor nodes are usually battery powered with limited energy sources, the system energy consumption must be minimized in order to extend the life time. Since the energy consumption of transceiver front ends is dominant in the whole sensor nodes, we focus on how to minimize energy consumption by the system level design. According to the applications, we analyze four types of RF architectures: on-off keying (OOK) transceiver, phase-shift keying (PSK) transceiver, quadrature amplitude modulation (QAM) transceiver, and frequency-shift keying (FSK) transceiver which are widely used in WSN and establish the related energy models for each kind of architecture, respectively. We connect the baseband parameters such as modulation level, data rate, bandwidth, and propagation distance. With the energy consumption of RF front end for WSN. Afterwards, through theoretical and numerical analysis in system level, we discuss and conclude how to design optimal energy-quality system in terms of various application scenarios.

1. Introduction

With the rapid development of wireless communication and low-power-embedded techniques, wireless sensor networks (WSNs) are widely used in many industrial and civilian application areas, including industrial process monitoring and control, machine status monitoring, environment and habitat monitoring, healthcare applications, home automation, and traffic control. It is obviously that the WSN services are becoming feasible and will bring a major change to our future daily lives as well as future human society. Although, most of the wireless sensor nodes are powered by batteries with limited energy source, it is very important to design an energy efficient system, and there has been a lot of attention paid to.

In recent years, different aspects of low-power techniques have been addressed for WSN. These include delay-controlled transmission scheme [1], energy efficient cooperative communication in WSN [2, 3], energy efficient modulation scaling [4–7], energy efficient routing schemes [8–10], power-management-based task scheduling for digital communication processors [11], cross-layer energy optimization [12]. However, in most of the prior work, the power dissipated in the RF and analog circuit is often ignored or over simplified to constant values. This may lead to erroneous energy evaluations, since the RF and analog sections process analog signals with high-frequency content and typically consume more energy compared to the digital part. According to [13], about 75% of the total power is dissipated in the RF front end. So, it is important to develop an accurate and comprehensive energy model for WSN RF front end. Such a model would definitely be helpful to develop a thorough tradeoff analysis between energy consumption and communication quality of wireless sensor networks.

Several system level energy models have also been proposed in recent years. For microsensor systems, the transceiver energy model considers the circuit start-up energy in addition to steady-state dissipated energy in [14]. Unfortunately, the energy consumption of every component

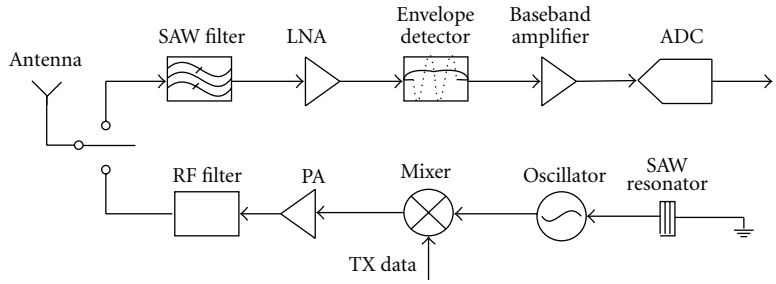

Figure 1: OOK transceiver [18–20].

is assumed to be constant; this is not suitable for real WSN application. Another high-level model was proposed in [15], which divides the circuitry power into two parts, one related to the instantaneous symbol rate and the other to the highest symbol rate. However, the dissipated circuit power is not only related to the symbol rate, but also to system parameters, such as signal peak-to-average Ratio (PAR) and signal bandwidth. In [6], a more comprehensive model is presented, however, most of the RF front-end components are still assumed to have constant power consumption, and the power model for power amplifier is gain dependent and does not take into account signal characteristics for instance signal PAR in M-QAM modulation. In order to accurately evaluate the effects of different communication system parameters on RF front-end energy consumption, we build a system level RF front-end energy model with QAM modulation for Wi-Fi application in the former works [16, 17] and tie the physical layer (PHY) parameters, such as bit error rate (BER), modulation level, bandwidth, and bit rate, to the RF circuit energy consumption. However, the prior work just considers one architecture or linear modulation scheme and has not considered the nonlinear system. The results can just be applied to the Wi-Fi system instead of WSN application. Since there are both linear and nonlinear RF front-ends architectures and modulation schemes widely used in WSN, to design an energy efficient system, we should not consider just one architecture or only linear modulation. For various applications, the optimal architecture or modulation scheme may be different. For instance, it is shown in [17] that the energy efficiency for 4QAM is higher than 16QAM with respect to long distance transmission. But 4QAM still be superior compared with other modulation schemes such as OOK modulation, FSK modulation, and PSK modulation? These problems should be clarified.

To design the energy efficient systems suitable for various WSN applications, we must know the available RF front-end architectures used in WSN nodes. In this paper, we develop the energy models for four types of RF front-ends architectures with OOK, PSK, QAM, and FSK modulation, respectively, which are popular in WSN nodes. We consider the effects of BER, PAR, modulation level, bandwidth, data rate and the transmission distance, and so forth in our energy models. And based on the energy models, we first theoretically compare the energy performance of different modulation schemes for different WSN applications in system level. For instance, we compare the energy performance of OOK, BPSK, and 2FSK modulation schemes for narrow bandwidth and low data rate application; QPSK, 4FSK, and 8QAM modulation schemes for medium bandwidth and medium data rate application; 16QAM, 32QAM, and 64QAM modulation schemes are considered for wide bandwidth and high data rate application. At last, we give the most energy efficient modulation scheme for different scenarios and summarize how to design the energy efficient system.

The remainder of this paper is organized as follows. Section 2 describes four RF front-end architectures widely used in the WSN nodes. The power models for the four RF front-ends are described in Section 3. In Section 4, we theoretically prove the most energy efficient modulation schemes and discuss the system design with various WSN applications. Finally conclusions are drawn in Section 5.

2. Typical RF Architectures for WSN Nodes

In order to design an energy efficient system, we must understand the RF architectures of the WSN nodes. In this section, we choose four typical RF architectures with different classes of PA for WSN nodes. There are two types of PA used in these architectures, which are the linear PA (e.g., Class A) and the nonlinear PA (e.g., Class E). The linear PA is adopted in linear modulation systems, such as OOK, PSK, and QAM, whereas the nonlinear PA would be employed in the nonlinear modulation systems, for example FSK modulation.

For the linear modulation, the OOK transceiver has the simplest architecture, which is shown in Figure 1. Direct-conversion transmitter is used in the OOK transceiver architecture. Digital baseband signal is mixed with carrier generated by the crystal and upconverted to RF band. Besides, in the receiver, the signal received from antenna is filtered by the SAW filter, amplified by low noise amplifier (LNA), demodulated by the envelope detector, and amplified by the baseband amplifier. Finally the original data are recovered by analog-to-digital converter (ADC). Noncoherent demodulation is applied in the receiver, which eliminates the mixer and reduces the overall size and power consumption.

The architecture of PSK transceiver is more complex than OOK transceiver, which is shown in Figure 2. The direct-conversion transmitter is also adopted in the PSK system, in

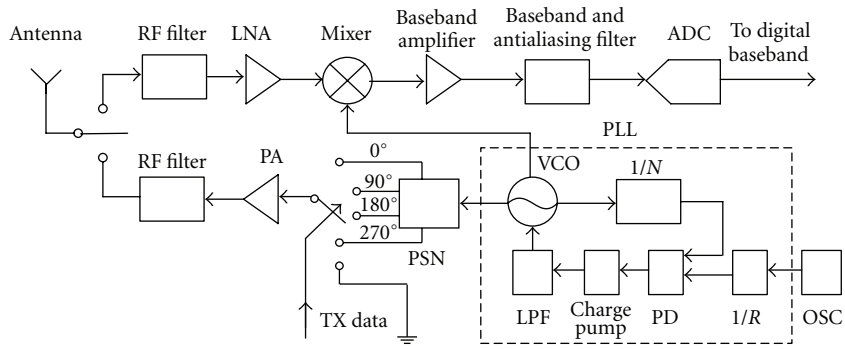

Figure 2: PSK transceiver [18, 19, 21].

which the phase modulation is accomplished by the phase-shifting-network (PSN) controlled by digital baseband signal. The modulation signal is transmitted directly to the PA without crossing the mixer. The heterodyne low-IF receiver is adopted in PSK systems. The main components in the receiver signal chain are the RF filter, LNA, downconversion mixer, baseband amplifier, baseband, and antialiasing filter, and ADC.

Figure 3 describes the RF front end of QAM system, which also employs the same receiver and direct-conversion transmitter. The main components of the analog signal chain of the transmitter are digital-to-analog converter (DAC), reconstruction filter, upconversion mixer, power amplifier (PA), and RF filter.

Besides, for the nonlinear modulation, the architecture of FSK transceiver is shown in Figure 4. Direct-conversion transmitter is adopted in FSK system too. The carriers in different frequencies are also generated by phase-locked loop (PLL) and controlled by the baseband signal. Then, the following processes are the same as the PSK system. The coherent demodulation is applied in the receiver. Note that there is just one pair of mixers in the transmitter and receiver active at the same time for the purpose of low power.

Generally speaking, the power efficiency of linear PA is lower than that of the nonlinear PA, while the bandwidth efficiency of linear modulation is higher than that of nonlinear modulation. For instance, according to [24], the bandwidth for PSK is

$$\mathrm{BW}_{\mathrm{MPSK}} = \frac{1+\alpha}{b} R_b, \tag{1}$$

where α denotes the roll-off factor of the pulse-shaping filter, b is the modulation level, and R_b denotes data rate. The bandwidth of MQAM is equal to MPSK. However, the bandwidth of FSK modulation can be expressed as

$$\mathrm{BW}_{\mathrm{MFSK}} = \frac{2^b + 3}{2 \cdot b} \cdot R_b. \tag{2}$$

Since $0 \le \alpha \le 1$ and $b \ge 1$, if the data rate is equal, it is obvious that $(1+\alpha)/b < (2^b+3)/2b$. So we can conclude that for the same modulation level, PSK and QAM have higher bandwidth efficiency than FSK.

3. System Level Power Models

To minimize the total energy consumption of a transceiver, it is essential to develop accurate energy models for all the key signal processing blocks. In the former work [16], we develop the energy models of RF front-end for Wi-Fi application and give the power consumption of the main components. As an extension work, in this work, we establish energy models for WSN nodes with both linear and nonlinear PAs. Since most power parameters of the analog blocks except PA are hard to be adjusted in WSN for low-power purpose, we assume that the power consumption of WSN nodes except PA is constant. As the power consumption of PA is dominant [13], we focus on it first.

The power consumption of PA can be divided into two parts: signal transmission power which is delivered to the antenna and dissipated power which is consumed by the electronic circuits. The transmission power P_{out} is proportional to the detected signal power P_{detected} at the receiver, the antenna gain, and the propagation distance. Assuming free space propagation at distance d, the radiated power P_{out} is given by

$$P_{\mathrm{detected}} = \frac{P_{\mathrm{out}} G_t G_r \lambda^2}{(4\pi)^2 d^2 L}, \tag{3}$$

where, G_t, G_r, λ, and d are transmitter and receiver antenna gains, carrier wavelength, and the transmission distance, respectively. L is the system loss factor not related to propagation. Note that the path loss factor equals 2 in this paper but other values can also be chosen.

According to [25], the efficiency of Class A PA is defined as

$$\eta = \frac{P_{\mathrm{out}}}{P_{\mathrm{PA}}} = \frac{K}{\mathrm{PAR}}, \tag{4}$$

where P_{PA} is the total power consumed by PA, K is a constant, and we choose $K = 0.5$ in this paper. So, we can get

$$P_{\mathrm{PA}} = \frac{P_{\mathrm{out}}}{K} \cdot \mathrm{PAR}. \tag{5}$$

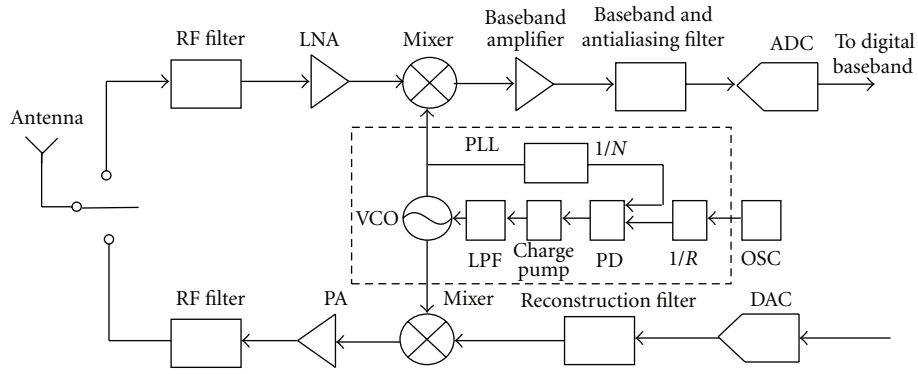

Figure 3: QAM transceiver [18, 19, 22].

According to [24, 26], the BER for OOK and QPSK modulation schemes are as follows:

$$\begin{aligned}
\text{OOK}: \ \text{BER}_{\text{OOK}} &= Q\left(\sqrt{\frac{P_{\text{detected}}}{2N}}\right),\\
\text{BPSK}: \ \text{BER}_{\text{BPSK}} &= Q\left(\sqrt{\frac{2P_{\text{detected}}}{N}}\right),\\
\text{QPSK}: \ \text{BER}_{\text{QPSK}} &= Q\left(\sqrt{\frac{2P_{\text{detected}}}{N}}\right),\\
\text{MPSK}: \ \text{BER}_{\text{MPSK}} &= \frac{2}{b}Q\left(\sqrt{\frac{4P_{\text{detected}}}{N}}\cdot\sin\left(\frac{\pi}{2^{b+1}}\right)\right),
\end{aligned} \tag{6}$$

where N is the noise power and b is the modulation level; $b = \log_2 M$. And $Q(\cdot)$ function is given by

$$Q(x) = \frac{1}{\sqrt{2\pi}}\int_x^{\infty} \mathrm{e}^{-y^2/2}dy. \tag{7}$$

So, the power consumption for the class A PA for OOK, BPSK, QPSK, and MPSK modulation can be written as

$$P_{\text{PA\_OOK}} = \frac{32\pi^2 d^2 L}{G_t G_r \lambda^2 K}\cdot N\cdot \text{PAR}\cdot\left[Q^{-1}(\text{BER})\right]^2, \tag{8}$$

$$P_{\text{PA\_BPSK}} = \frac{8\pi^2 d^2 L}{G_t G_r \lambda^2 K}\cdot N\cdot \text{PAR}\cdot\left[Q^{-1}(\text{BER})\right]^2, \tag{9}$$

$$P_{\text{PA\_QPSK}} = \frac{8\pi^2 d^2 L}{G_t G_r \lambda^2 K}\cdot N\cdot \text{PAR}\cdot\left[Q^{-1}(\text{BER})\right]^2, \tag{10}$$

$$P_{\text{PA\_MPSK}} = \frac{4\pi^2 d^2 L}{G_t G_r \lambda^2 K}\cdot N\cdot \text{PAR}\cdot\left[\frac{Q^{-1}((b\cdot\text{BER})/2)}{\sin(\pi/2^{b+1})}\right]^2, \tag{11}$$

where, $Q^{-1}(\cdot)$ is the inverse function of $Q(\cdot)$; PAR = 1 for PSK modulation.

In our former work [17], the power consumption of PA in MQAM systems has been proposed as

$$\begin{aligned}
&P_{\text{PA_MQAM}}\\
&\quad= \frac{16\pi^2 d^2 L}{3G_t G_r \lambda^2 K}\left(2^b-1\right)\cdot N\\
&\qquad\cdot\left[Q^{-1}\left(\frac{1}{4}\left(1-\frac{1}{2^{b/2}}\right)^{-1}\cdot b\cdot\text{BER}\right)\right]^2\cdot\text{PAR}_{\text{MQAM}}.
\end{aligned} \tag{12}$$

For the nonlinear modulation, the BER expression for MFSK modulation is shown in [24]:

$$\text{BER}_{\text{MFSK}} = \frac{2^b-1}{b}Q\left(\sqrt{\frac{b\cdot P_{\text{detected}}}{N}}\right). \tag{13}$$

So, the power model for Class E PA [27] with FSK modulation is as follow:

$$P_{\text{out\_MFSK}} = \frac{16\pi^2 d^2 L}{G_t G_r \lambda^2}\cdot\frac{N}{b}\cdot\left[Q^{-1}\left(\frac{b\cdot\text{BER}}{2^b-1}\right)\right]^2, \tag{14}$$

$$\begin{aligned}
&P_{\text{PA_MFSK}}\\
&\quad= \left(1+\frac{R_{\text{on}}}{V_{\text{DD}}^2}\cdot\frac{Q_{\text{Lf}}}{Q_{\text{Lf}}-Q_{\text{f}}}\cdot F\cdot P_{\text{out_MFSK}}+\frac{G}{Q_{Ls}}\right)\\
&\qquad\cdot\left(1-\frac{Q_{\text{f}}}{Q_{\text{Lf}}}\right)^{-1}\cdot P_{\text{out_MFSK}},
\end{aligned} \tag{15}$$

where Q_{f} and Q_{Lf} are the quality factors of output LC filter with or without the load. Q_{Ls} is the quality factor of shunt inductor. R_{on} and V_{DD} are the switch resistance and supply voltage of the Class E PA. F and G are the power dissipation coefficients, and $F = 2.3$ and $G = 1.7$ are chosen to make the PA operate at the highest efficiency [27]. $P_{\text{out\_MFSK}}$ is the output power of Class E PA.

As the energy consumption for the RF front end includes the energy consumption of PA and other blocks; the energy per bit can be expressed as

$$E_{\text{bit}} = \frac{P_E}{(b\cdot R_s)} + \frac{P_{\text{PA}}}{(b\cdot R_s)}, \tag{16}$$

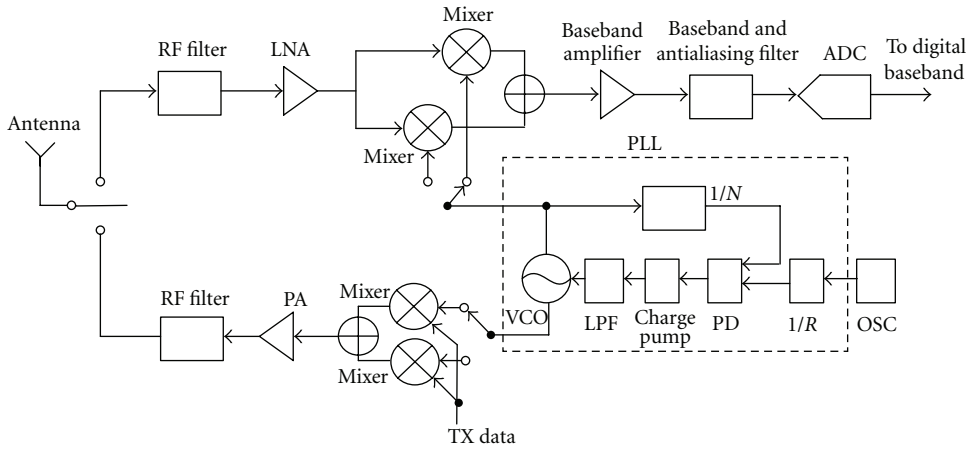

Figure 4: FSK transceiver [18, 19, 23].

Table 1: Simulation parameters.

$f = 2.4\,\text{GHz}$	$Q_f = 10$	$\alpha = 0.2$
$\text{BER} = 1e-3$	$Q_{Lf} = 100$	$P_{E\_OOK} = 72.35e-3\,\text{W}$
$L = 1.25$	$Q_{Ls} = 10$	$P_{E\_BPSK} = 126.85e-3\,\text{W}$
$G_r = G_t = 1$	$R_{on} = 0.05\,\Omega$	$P_{E\_QPSK} = 126.85e-3\,\text{W}$
$K = 0.5$	$V_{DD} = 3.3\,\text{V}$	$P_{E\_8PSK} = 126.85e-3\,\text{W}$
$N_0 = 2e-16\,\text{W/Hz}$	$F = 2.3$	$P_{E\_MFSK} = 147.85e-3\,\text{W}$
$\text{PAR}_{\text{roll\_off}} = 5\,\text{dB}$	$G = 1.7$	$P_{E\_MQAM} = 165.75e-3\,\text{W}$

where E_{bit} denotes the energy per bit consumed by RF front end, P_E is the power consumption of the RF circuits except PA and R_s denotes the symbol rate.

4. Energy Evaluations for Different Applications

In this part, we analyze and model the energy consumption of the four types of RF front ends with different modulation schemes for WSN applications, which is an extension of our former energy modeling work [16]. According to the data rate and bandwidth requirements, we divide the applications into six types, namely, narrow bandwidth (less than 50 KHz), low data rate (less than 50 Kbps), medium bandwidth (from 50 KHz to 500 KHz), middle data rate (from 50 Kbps to 500 Kbps), wide bandwidth (above 500 KHz), and high data rate (above 500 Kbps). And in this paper, we assume the transmission distance is within 150 meters. So, the values of $d^2 \cdot \text{BW}$ and $d^2 \cdot R_s$ are less than 1.125×10^9 for narrow bandwidth and low data rate application and less than 1.125×10^{11} for medium bandwidth and middle data rate application, respectively, and we assume the values of $d^2 \cdot \text{BW}$ and $d^2 \cdot R_s$ are less than 1.125×10^{13} for wide bandwidth and high data rate application. For low bandwidth or low data rate communication system, we consider OOK, BPSK, and 2FSK modulation schemes, for middle bandwidth or middle data rate instance, we study QPSK, 4FSK, and 8QAM, and we adopt 16QAM, 32QAM, and 64QAM for high bandwidth or high data rate application. The related parameter values used in our simulation are listed in Table 1 [15, 16].

Since bandwidth (BW) is a precious resource in most communication system, in this paper we assume it is constant, and the data rate can be adjusted only by changing the modulation level. Also we assume pulse shaping technique is used in the system to remove intersymbol interference (ISI) and pulse-shaping filter roll-off factor α equals 0.2. The power consumption values P_E for every modulation scheme are referred from the data sheets of the RF or analog components by TI or RFMD companies. Note that P_E can be set as different values but the trends of E_{bit} are similar.

4.1. Narrow-Bandwidth System. We choose OOK, BPSK and 2FSK modulation for low-bandwidth system, and the relations between data rate and bandwidth are as follows:

$$R_{b\_\text{OOK}} = R_{b\_\text{BPSK}} = \frac{\text{BW}}{1+\alpha}, \qquad \text{R}_{b\_\text{2FSK}} = \frac{2}{5}\text{BW}. \tag{17}$$

According to (8), (9), (15), and (16), energy per bit for OOK, BPSK, and 2FSK can be expressed, respectively, as

$$E_{\text{bit\_OOK}} = \frac{(1+\alpha)\cdot P_{E\_\text{OOK}}}{\text{BW}} + \frac{32\pi^2(1+\alpha)\cdot L\cdot d^2\cdot BW\cdot N_0}{\text{BW}\cdot G_t\cdot G_r\cdot\lambda^2\cdot K} \cdot \text{PAR}\cdot\left[Q^{-1}(\text{BER})\right]^2,$$

$$E_{\text{bit\_BPSK}} = \frac{(1+\alpha)P_{E\_\text{BPSK}}}{\text{BW}} + \frac{8\pi^2(1+\alpha)L\cdot d^2\cdot\text{BW}\cdot N_0}{\text{BW}\cdot G_t\cdot G_r\cdot\lambda^2\cdot K} \cdot \text{PAR}\cdot\left[Q^{-1}(\text{BER})\right]^2,$$

$$E_{\text{bit\_2FSK}} = \frac{5P_{E\_2\text{FSK}}}{2\text{BW}} + \left(1 - \frac{Q_f}{Q_{Lf}}\right)^{-1} \cdot \frac{40\pi^2 L \cdot d^2 \cdot \text{BW} \cdot N_0}{\text{BW} \cdot G_t G_r \lambda^2} \cdot \text{PAR}\left[Q^{-1}(\text{BER})\right]^2 \cdot \left(\begin{array}{l} 1 + \dfrac{R_{on}}{V_{DD}^2} \cdot \dfrac{Q_{Lf}}{Q_{Lf} - Q_f} \cdot F \\ \cdot \dfrac{16\pi^2 L d^2 N_0 \cdot \text{BW}}{G_t G_r \lambda^2} \cdot \text{PAR} \\ \cdot \left[Q^{-1}(\text{BER})\right]^2 + \dfrac{G}{Q_{Ls}} \end{array} \right). \tag{18}$$

4.1.1. BPSK versus OOK. Firstly, we compare the energy per bit of BPSK and OOK modulation scheme.

Let

$$\begin{aligned} F_1(d^2, \text{BW}) &= E_{\text{bit\_BPSK}} - E_{\text{bit\_OOK}} \\ &= \frac{(1+\alpha) \cdot (P_{E\_\text{BPSK}} - P_{E\_\text{OOK}})}{\text{BW}} \\ &\quad - \frac{24\pi^2(1+\alpha) \cdot L \cdot d^2 \cdot \text{BW} \cdot N_0}{\text{BW} \cdot G_t \cdot G_r \cdot \lambda^2 \cdot K} \\ &\quad \cdot \text{PAR} \cdot \left[Q^{-1}(\text{BER})\right]^2. \end{aligned} \tag{19}$$

If $F_1(d^2, \text{BW}) < 0$, it means $E_{\text{bit\_BPSK}} < E_{\text{bit\_OOK}}$, then we can solve the above inequality and get the solution as

$$d^2 \cdot \text{BW} > \frac{(P_{E\_\text{BPSK}} - P_{E\_\text{OOK}}) \cdot G_t \cdot G_r \cdot \lambda^2 \cdot K}{24\pi^2 L \cdot N_0 \cdot \text{PAR} \cdot \left[Q^{-1}(\text{BER})\right]^2}. \tag{20}$$

We set the values of the parameters as listed in Table 1, then

$$d^2 \cdot \text{BW} > 2.1844e + 8. \tag{21}$$

If $F_1(d^2, \text{BW}) = 0$, it means OOK and BPSK modulation scheme has the same energy efficiency. We can also get the solution as $d^2 \cdot \text{BW} = 2.1844e + 8$.

If $F_1(d^2, \text{BW}) > 0$, it means $E_{\text{bit\_BPSK}} > E_{\text{bit\_OOK}}$. Similarly, we can get the solution as $d^2 \cdot \text{BW} < 2.1844e + 8$.

From the analysis above and the restriction of $d^2 \cdot \text{BW} < 1.125e + 9$, we can conclude that when $1.125e + 9 > d^2 \cdot \text{BW} > 2.1844e + 8$, BPSK modulation scheme is more energy efficient than OOK modulation scheme, and when $d^2 \cdot \text{BW} < 2.1844e + 8$, OOK performs better.

4.1.2. 2FSK versus OOK. Secondly, let us compare the energy per bit of 2FSK and OOK modulation. Suppose

$$\begin{aligned} \xi &= \left(1 - \frac{Q_f}{Q_{Lf}}\right)^{-1} \cdot \frac{16\pi^2 L \cdot N_0}{G_t G_r \lambda^2} \cdot \text{PAR} \cdot \left[Q^{-1}(\text{BER})\right]^2, \\ F_2(d^2, \text{BW}) &= E_{\text{bit\_2FSK}} - E_{\text{bit\_OOK}} \\ &= \frac{(5/2)P_{E\_2\text{FSK}} - (1+\alpha) \cdot P_{E\_\text{OOK}}}{\text{BW}} \\ &\quad - \frac{2(1+\alpha)\xi \cdot d^2 \cdot \text{BW}}{\text{BW} \cdot K} \\ &\quad \cdot \left(1 - \frac{Q_f}{Q_{Lf}}\right) + \frac{5}{2}\frac{d^2 \cdot \text{BW}}{\text{BW}} \cdot \xi \\ &\quad \cdot \left(1 + \frac{R_{on}}{V_{DD}^2} \cdot F \cdot \xi \cdot d^2 \cdot \text{BW} + \frac{G}{Q_{Ls}}\right). \end{aligned} \tag{22}$$

Let $A = (5/2)(R_{on}/V_{DD}^2) \cdot F \cdot \xi^2$, $B = (5/2)\xi \cdot (1 + G/Q_{Ls}) - ((2(1+\alpha) \cdot \xi)/K) \cdot (1 - Q_f/Q_{Lf})$, and $C = (5/2)P_{E\_2\text{FSK}} - (1+\alpha) \cdot P_{E\_\text{OOK}}$, then

$$F_2(d^2, \text{BW}) = \frac{1}{\text{BW}} \cdot \left(A \cdot (d^2 \cdot \text{BW})^2 + B \cdot (d^2 \cdot \text{BW}) + C\right). \tag{23}$$

Assume $F_2(d^2, \text{BW}) = 0$, which means 2FSK and OOK modulation scheme has the same energy efficiency, we can solve the above function and get the roots $d^2 \cdot \text{BW} = (-B \pm \sqrt{B^2 - 4A \cdot C})/2A$. We set the values of the parameters as listed in Table 1 and calculate the root values of $d^2 \cdot \text{BW}$ as:

$$\begin{aligned} X_1 &= \frac{-B - \sqrt{B^2 - 4A \cdot C}}{2A} = 6.2616e + 8, \\ X_2 &= \frac{-B + \sqrt{B^2 - 4A \cdot C}}{2A} = 2.5369e + 13. \end{aligned} \tag{24}$$

Since $A > 0$, if $6.2616e + 8 < d^2 \cdot \text{BW} < 2.5369e + 13$, then $E_{\text{bit\_2FSK}} - E_{\text{bit\_OOK}} < 0$, and considering the restriction of $d^2 \cdot \text{BW}$, we can get the result that when $6.2616e + 8 < d^2 \cdot \text{BW} < 1.125e + 9$, 2FSK modulation scheme is more energy efficient than OOK modulation scheme. If $d^2 \cdot \text{BW} < 6.2616e + 8$, then $E_{\text{bit\_2FSK}} - E_{\text{bit\_OOK}} > 0$; it means OOK modulation scheme is more energy efficient than 2FSK modulation scheme.

4.1.3. 2FSK versus BPSK. Similarly, we can compare the energy performance of 2FSK and BPSK modulation. If $2.2465e+9 < d^2 \cdot \text{BW} < 5.1002e+12$, then $E_{\text{bit\_2FSK}} - E_{\text{bit\_BPSK}} < 0$, but considering the restriction of $d^2 \cdot \text{BW}$, we find that $2.2465e + 9 < d^2 \cdot \text{BW} < 5.1002e + 12$ is not suitable for narrow bandwidth application and has to be abandoned. If $d^2 \cdot \text{BW} < 2.2465e + 9$ or $d^2 \cdot \text{BW} > 5.1002e + 12$, then $E_{\text{bit\_2FSK}} - E_{\text{bit\_BPSK}} > 0$, and with the consideration of the value restriction of $d^2 \cdot \text{BW}$, we can conclude that when $d^2 \cdot \text{BW} < 1.125e + 9$, BPSK is more energy efficient than 2FSK.

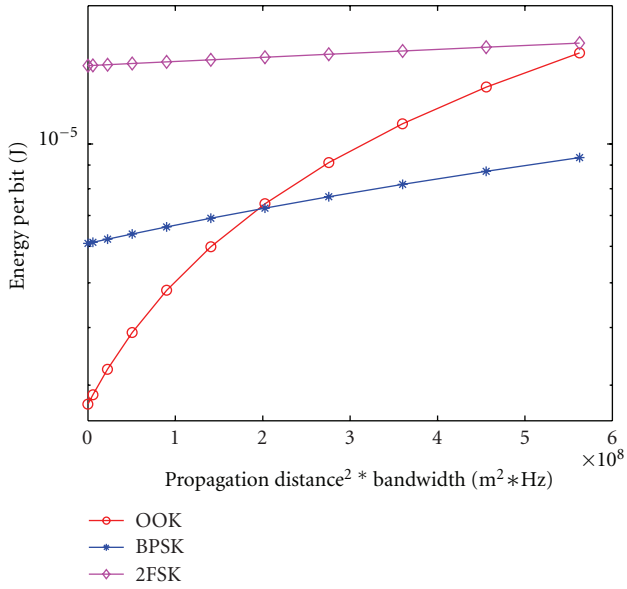

Figure 5: Energy per bit for different RF front-end architecture in narrow-bandwidth application, BW = 25 KHz and $d = (0\ 150]$ m.

4.1.4. Example and Discussion. To verify the above theoretical analysis, we choose BW = 25 KHz as an example and draw Figure 5. From Figure 5 we can see that the OOK modulation scheme has the lowest energy consumption when $d^2 \cdot \mathrm{BW}$ is small. This is because when $d^2 \cdot \mathrm{BW}$ is small, the analog circuit energy consumption is dominant instead of PA. The OOK modulation system is much simpler than others, and thus OOK has the best energy performance. But, with the increase of transmission distance, PA consumes much more energy compared with other RF blocks. When $d^2 \cdot \mathrm{BW}$ increases to a certain value, BPSK modulation becomes the most energy efficient. 2FSK has higher energy consumption than BPSK; this is because when the bandwidth is fixed, according to (1) and (2), the data rate of 2FSK modulation is much slower than BPSK. From Figure 5 we can also see that the energy consumption of 2FSK modulation scheme changes much slower than that of OOK and BPSK, this owes to the high efficiency of Class E PA used in 2FSK system.

From the above example and theoretical analysis, we can conclude that when $d^2 \cdot \mathrm{BW} < 2.1844e + 8$, OOK modulation scheme is high energy efficient; when $2.1844e + 8 < d^2 \cdot \mathrm{BW} < 1.125e + 9$, BPSK modulation scheme has the best energy performance.

4.2. Low Data Rate System. For low data rate application, the bandwidths of OOK, BPSK, and 2FSK modulation can be expressed as follows:

$$\mathrm{BW}_{\mathrm{OOK}} = \mathrm{BW}_{\mathrm{BPSK}} = (1+\alpha)R_b,$$
$$\mathrm{BW}_{\mathrm{2FSK}} = \frac{5}{2}R_b. \tag{25}$$

So, the energy per bit for OOK, BPSK, and 2FSK can be expressed, respectively, as

$$\begin{aligned}
E_{\mathrm{bit_OOK}} &= \frac{P_{E_\mathrm{OOK}}}{R_b} + \frac{32\pi^2 L \cdot d^2 \cdot N_0 \cdot (1+\alpha)R_b}{R_b \cdot G_t \cdot G_r \cdot \lambda^2 \cdot K} \\
&\quad \cdot \mathrm{PAR} \cdot \left[Q^{-1}(\mathrm{BER})\right]^2, \\
E_{\mathrm{bit_BPSK}} &= \frac{P_{E_\mathrm{BPSK}}}{R_b} + \frac{8\pi^2 L \cdot d^2 \cdot N_0 \cdot (1+\alpha)R_b}{R_b \cdot G_t \cdot G_r \cdot \lambda^2 \cdot K} \\
&\quad \cdot \mathrm{PAR} \cdot \left[Q^{-1}(\mathrm{BER})\right]^2, \\
E_{\mathrm{bit_2FSK}} &= \frac{P_{E_\mathrm{2FSK}}}{R_b} + \frac{Q_{\mathrm{Lf}}}{Q_{\mathrm{Lf}} - Q_{\mathrm{f}}} \cdot \frac{40\pi^2 L \cdot d^2 \cdot N_0 \cdot R_b}{R_b \cdot G_t G_r \lambda^2} \\
&\quad \cdot \left[Q^{-1}(\mathrm{BER})\right]^2 \cdot \left(\begin{array}{l} 1 + \dfrac{R_{\mathrm{on}}}{V_{\mathrm{DD}}^2} \cdot \dfrac{Q_{\mathrm{Lf}}}{Q_{\mathrm{Lf}} - Q_{\mathrm{f}}} \cdot F \\ \cdot \dfrac{40\pi^2 L \cdot d^2 \cdot N_0 \cdot R_b}{G_t G_r \lambda^2} \\ \cdot \left[Q^{-1}(\mathrm{BER})\right]^2 + \dfrac{G}{Q_{Ls}} \end{array} \right).
\end{aligned} \tag{26}$$

According to (26), Figure 6 shows the energy per bit with OOK, BPSK, and 2FSK modulation when the data rate is 25 Kbps. From Figure 6 we can see that for a given data rate, the OOK modulation scheme has the lowest energy consumption when the transmission distance is short. This is because when the transmission distance is short, which means $d^2 \cdot R_b$ is small, the analog circuit energy consumption is dominant instead of PA. The OOK modulation system is much simpler than others and thus OOK has the best energy performance. But with the increase of $d^2 \cdot R_b$, PA consumed much more energy compared with other RF blocks. When $d^2 \cdot R_b$ increases to a certain value, BPSK modulation becomes the most energy efficient. However, when the $d^2 \cdot R_b$ is large enough, 2FSK modulation scheme becomes the best choice; this owes to the high efficiency of Class E PA used in 2FSK system.

With the similar method used to analyze the low-bandwidth system, we can conclude that when $d^2 \cdot R_b < 1.8203e + 8$, OOK modulation scheme is the most energy efficient; when $1.8203e + 8 < d^2 \cdot R_b < 4.2214e + 8$, BPSK modulation scheme has the best energy performance; if $4.2214e + 8 < d^2 \cdot R_b < 1.125e + 9$, 2FSK modulation scheme consumes the least energy.

4.3. Medium-Bandwidth System. For medium-bandwidth application, we consider QPSK, 8QAM, and 4FSK modulation scheme. According to (1), (10), (12), (15), and (16), Figure 7 shows the energy per bit with QPSK, 8QAM, and 4FSK modulation when the bandwidth BW is 250 KHz. From Figure 7 we can see that when the transmission distance is short, which means $d^2 \cdot \mathrm{BW}$ is small, 8QAM modulation scheme has the lowest energy consumption. This is because 8QAM has the highest data rate and saves the active time. With the increase of the transmission distance, which means the value of $d^2 \cdot \mathrm{BW}$ will become larger, QPSK modulation scheme performs best. On the other hand, 4FSK modulation

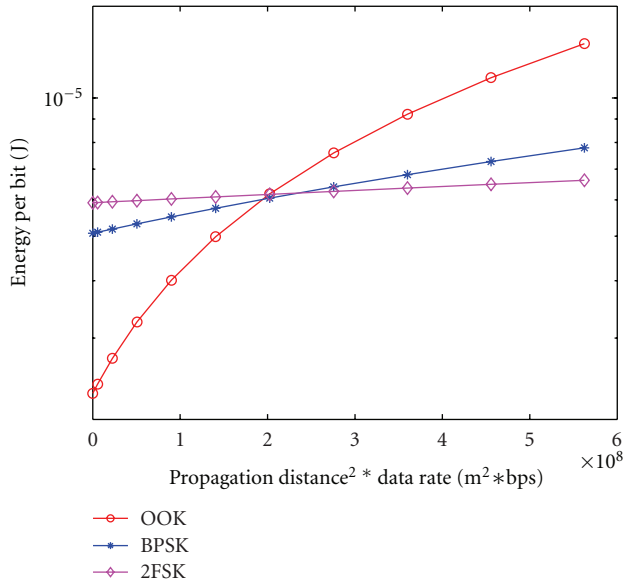

Figure 6: Energy per bit for different RF front-end architecture in low data rate application, R_b = 25 Kbps and d = (0 150] m.

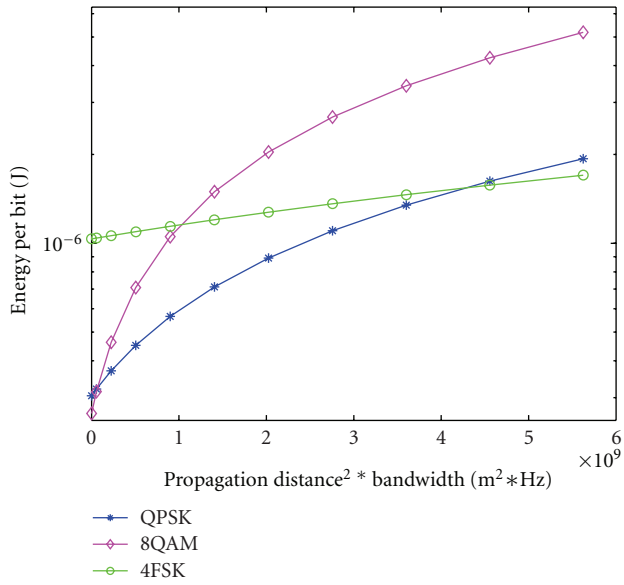

Figure 7: Energy per bit for different RF front-end architecture in medium-bandwidth application and BW = 250 KHz, d = (0 150] m.

system has the highest energy consumption for small $d^2 \cdot \mathrm{BW}$, which comes from the fact that for a given transmission bandwidth, the data rate of 4FSK modulation is lower than QPSK and 8QAM. But with the increase of $d^2 \cdot \mathrm{BW}$, the energy consumption of 4FSK increases much slower than the other two modulation schemes; this is because the nonlinear PA used in 4FSK modulation system has higher efficiency. For large $d^2 \cdot \mathrm{BW}$, the advantage of the high efficiency of nonlinear PA is obvious.

With the similar method to analyze the low-bandwidth system, we can compare the energy performance of 4FSK, QPSK, and 8QAM modulation. When $d^2 \cdot \mathrm{BW} < 5.8472e + 7$, 8QAM modulation scheme is the most energy efficient. When $5.8472e+7 < d^2 \cdot \mathrm{BW} < 5.2965e+9$, QPSK modulation scheme is the best choice. If $5.2965e + 9 < d^2 \cdot \mathrm{BW} < 1.125e + 11$, then 4FSK is superior.

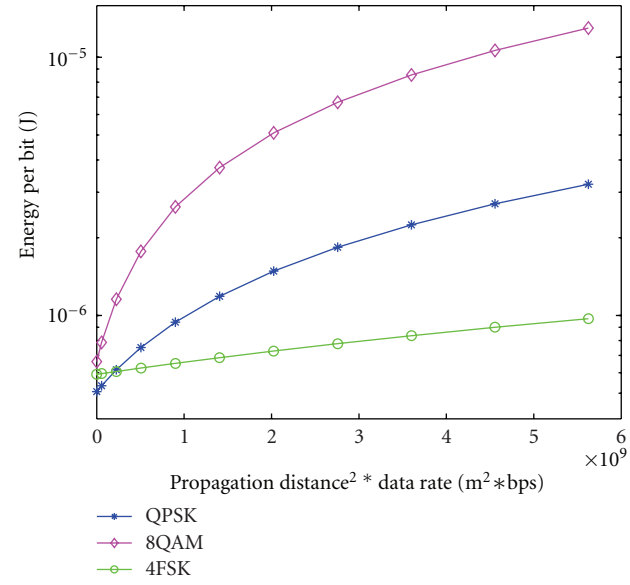

Figure 8: Energy per bit for different RF front-end architecture in medium data rate application, R_b = 250 Kbps, d = (0 150] m.

4.4. Medium Data Rate System. For medium data rate application, we also consider QPSK, 8QAM, and 4FSK modulation scheme; Figure 8 shows the energy per bit with QPSK, 8QAM and 4FSK modulation when the data rate is 250 Kbps. From Figure 8 we can see when $d^2 \cdot R_b$ is small, QPSK modulation scheme is the most energy efficient. This is because when $d^2 \cdot R_b$ is small, the analog circuit energy consumption is dominant instead of PA. The QPSK modulation system is much simpler than others, and thus QPSK has the best energy performance. But with the increase of $d^2 \cdot R_b$, the energy consumption of 4FSK increases much slower than the other two modulation schemes; this is because the nonlinear PA used in 4FSK modulation system has higher efficiency. For large $d^2 \cdot R_b$, the advantage of the high efficiency of nonlinear PA is obvious.

With the similar method to analyze the low data rate system, we can compare the energy performance of 4FSK, QPSK, and 8QAM modulation. When $d^2 \cdot R_b < 6.0875e + 8$, QPSK modulation scheme is most energy efficient. When $6.0875e + 8 < d^2 \cdot R_b < 1.125e + 11$, 4FSK modulation scheme is the best choice.

4.5. Wide-Bandwidth System. We choose QAM modulation scheme with high modulation level for wide-bandwidth application and analyze the energy performance. In this paper, we adopt 16QAM, 32QAM and 64QAM.

According to (1), (12), and (16), we draw Figure 9 which illustrates the energy consumption per bit for different level

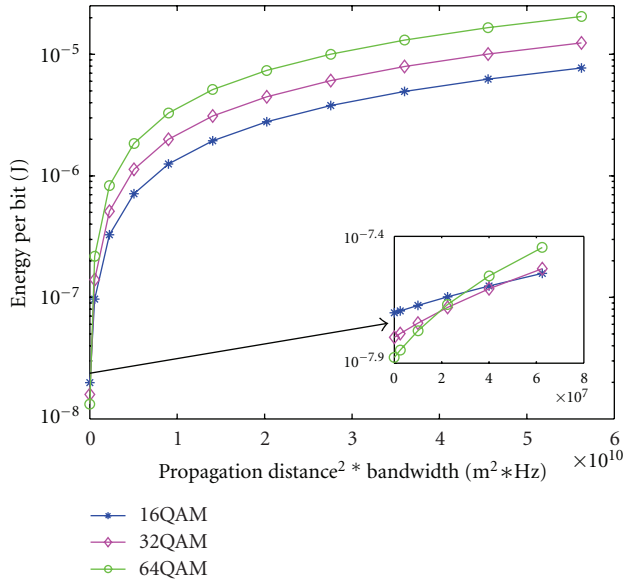

Figure 9: Energy per bit for different RF front-end architecture in wide-bandwidth application, BW = 2.5 MHz and d = (0 150] m.

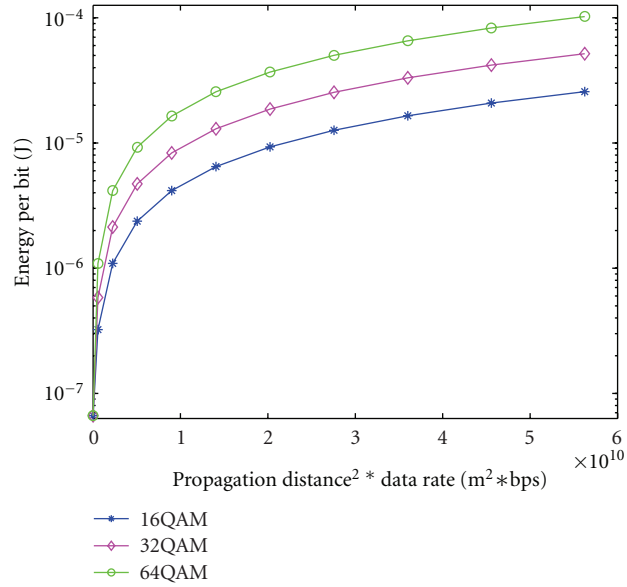

Figure 10: Energy per bit for different RF front-end architecture in high data rate application, R_b = 2.5 Mbps, d = (0 150] m.

Table 2: Styles energy efficient system for same bandwidth.

Modulation scheme	$d^2 \cdot$ BW		
	Large	Medium	Small
Bandwidth			
Wide	16QAM	16QAM	64QAM, 32QAM
Medium	4FSK, QPSK	QPSK	8QAM
Narrow	BPSK	BPSK, OOK	OOK

Table 3: Styles energy efficient system for same data rate.

Modulation scheme	$d^2 \cdot R_b$		
	Large	Medium	Small
Data rate			
High	16QAM	16QAM	16QAM
Medium	4FSK	4FSK	QPSK
Low	2FSK	BPSK	OOK

of QAM modulation. Here, we choose BW = 2.5 MHz as the example. From Figure 9 we can see that when $d^2 \cdot$ BW is small, higher modulation level scheme is more energy efficient. By contraries, for large $d^2 \cdot$ BW, lower modulation level performs better. This is because with the increase of modulation level, the energy consumption of RF circuits except PA will decrease, but the energy consumption of PA will increase. When $d^2 \cdot$ BW is small, the circuit energy consumption except PA is dominant, so the total energy consumption will decrease with the increase of modulation level. But for large $d^2 \cdot$ BW, the energy consumption of PA becomes dominant, so the total energy consumption will increase with the increase of modulation level.

With the same method used to analyze the low-bandwidth system, we obtain that when $d^2 \cdot \text{BW} < 1.2675e{+}7$, 64QAM is superior; when $1.2675e+7 < d^2 \cdot \text{BW} < 3.3161e+7$, 32QAM is the most energy efficient; when $d^2 \cdot \text{BW} > 3.3161e+7$, 16QAM has the best energy performance.

4.6. High Data Rate System. In this paper, we also adopt 16QAM, 32QAM, and 64QAM modulation scheme for high data rate application and analyze the energy performance.

According to (1), (12), and (16), we draw Figure 10 which illustrates the energy consumption per bit for different level of QAM modulation. Here, we choose R_b = 2.5 Mbps as the example. From Figure 10 we can see that lower modulation level scheme is more energy efficient. This is because with the increase of modulation level, the energy consumption of PA will increase. And as the data rate is same, the circuit energy consumption except PA is equal, so the total energy consumption will increase with the increase of modulation level.

4.7. Summary and Design Steps for Energy Efficient System. In the former sections, we evaluate the energy performance of different modulation schemes under different WSN applications. In reality, as to most of wireless communication systems, BW is fixed and cannot be adjusted. Then, in order to clearly illustrate the relationship among propagation distance, modulation scheme, and energy consumption, BW is assumed to be constant during numerical analysis in the former subsections. According to the theoretical analysis results, if substituting the values of BW or R_b that we assumed, some recommended modulation schemes for designing an energy efficient system are given and summarized in Tables 2 and 3. It is seen from Tables 2 and 3 that under different application scenario, the optimal modulation scheme is different. So when designing an energy efficient system, we should firstly understand the application requirement, such as bandwidth and data rate. Then, the

theoretical analysis results in this section can be utilized to find out the optimal modulation scheme and choose the corresponding RF front-end architecture.

5. Conclusion

In this paper, we describe four kinds of RF front-end architectures which are widely used in wireless sensor nodes. The comprehensive energy models for different WSN nodes are proposed and analyzed in details. Based on the theoretical and numerical analysis, we discuss how to choose the optimal modulation scheme in terms of different propagation distances and bandwidths or data rates, covering from low bandwidth or data rate to high bandwidth and data rate. According to our theoretical analysis, we find that if the bandwidth is the same, for narrow bandwidth systems, OOK is the most energy efficient for short range communication, and BPSK is optimal for long range communication; as to medium bandwidth systems, 8QAM performs best for short range communication, and QPSK is optimal for long range communication; as to wide bandwidth systems, 16QAM is the best for long distance communication. But if we assume the data rate is the same for different applications, the results may be slightly different. The simulation results have verified our conclusion. Finally, some conclusions on designing an energy efficient system are given.

Acknowledgments

This work was supported in part by the National Natural Science Foundation of China (no. 81101127), Shenzhen Basic Research Funds for Distinguished Young Scientists (no. JC201005270306A), and the development funds for Key Laboratory in Shenzhen (no. CXB201104220026A).

References

[1] X. Wang, Y. Ren, J. Zhao, Z. Guo, and R. Yao, "Energy efficient transmission protocol for UWB WPAN," in *Proceedings of the IEEE 60th Vehicular Technology Conference (VTC '04)*, pp. 5292–5296, Los Angeles, Calif, USA, September 2004.

[2] Z. Zhou, S. Zhou, S. Cui, and J. H. Cui, "Energy-efficient cooperative communication in a clustered wireless sensor network," *IEEE Transactions on Vehicular Technology*, vol. 57, no. 6, pp. 3618–3628, 2008.

[3] Z. Zhou, S. Zhou, J. H. Cui, and S. Cui, "Energy-efficient cooperative communication based on power control and selective single-relay in wireless sensor networks," *IEEE Transactions on Wireless Communications*, vol. 7, no. 8, pp. 3066–3079, 2008.

[4] S. Gao, L. Qian, D. R. Vaman, and Q. Qu, "Energy efficient adaptive modulation in wireless cognitive radio sensor networks," in *Proceedings of the IEEE International Conference on Communications (ICC '07)*, pp. 3980–3986, Scotland, UK, June 2007.

[5] Z. Yang, Y. Yuan, and J. He, "Energy aware data gathering based on adaptive modulation scaling in wireless sensor networks," in *Proceedings of the IEEE 60th Vehicular Technology Conference (VTC '04)*, pp. 2794–2798, Los Angeles, Calif, USA, September 2004.

[6] S. Cui, A. J. Goldsmith, and A. Bahai, "Modulation optimization under energy constraints," in *Proceedings of the International Conference on Communications (ICC '03)*, pp. 2805–2811, King of Prussia, Pa, USA, May 2003.

[7] T. Wang, W. Heinzelman, and A. Seyedi, "Minimization of transceiver energy consumption in wireless sensor networks with AWGN channels," in *Proceedings of the 46th Annual Allerton Conference on Communication, Control, and Computing*, pp. 62–66, Monticello, Ill, USA, September 2008.

[8] N. Uppu, B. V. S. S. Subrahmanyam, and R. Garimella, "Energy efficient routing technique for ad-hoc sensor networks [EERT]," in *Proceedings of the 3rd IEEE Sensors Applications Symposium (SAS '08)*, pp. 228–232, Atlanta, Ga, USA, February 2008.

[9] D. Li, X. Jia, and H. Liu, "Energy efficient broadcast routing in static ad hoc wireless networks," *IEEE Transactions on Mobile Computing*, vol. 3, no. 2, pp. 144–151, 2004.

[10] S. Mahfoudh and P. Minet, "An energy efficient routing based on OLSR in wireless ad hoc and sensor networks," in *Proceedings of the 22nd International Conference on Advanced Information Networking and Applications Workshops/Symposia (AINA '08)*, pp. 1253–1259, Ginowan, Japan, March 2008.

[11] K. Lahiri, A. Raghunathan, and S. Dey, "Communication-based power management," *IEEE Design and Test of Computers*, vol. 19, no. 4, pp. 118–130, 2002.

[12] S. Cui, R. Madan, A. J. Goldsmith, and S. Lall, "Cross-layer energy and delay optimization in small-scale sensor networks," *IEEE Transactions on Wireless Communications*, vol. 6, no. 10, pp. 3688–3699, 2007.

[13] M. Srivatsava, "Power-aware communication systems," in *Power-Aware Design Methodologies*, M. Rabaey, Ed., chapter 11, Kluwer Academic Publishers, Norwell, Mass, USA, 2002.

[14] A. Y. Wang, Seong Hwan Cho, C. G. Sodini, and A. P. Chandrakasan, "Energy efficient modulation and MAC for asymmetric RF microsensor systems," in *Proceedings of the International Symposium on Low Electronics and Design (ISLPED '01)*, pp. 106–111, Huntington Beach, Calif, USA, August 2001.

[15] C. Schurgers, O. Aberthorne, and M. B. Srivastava, "Modulation scaling for energy aware communication systems," in *Proceedings of the International Symposium on Low Power Electronics and Design (ISLPED '01)*, pp. 96–99, Huntington Beach, Calif, USA, August 2001.

[16] Y. Li, B. Bakkaloglu, and C. Chakrabarti, "A system level energy model and energy-quality evaluation for integrated transceiver front-ends," *IEEE Transactions on Very Large Scale Integration (VLSI) Systems*, vol. 15, no. 1, pp. 90–102, 2007.

[17] Y. Li, M. Reisslein, and C. Chakrabarti, "Energy-efficient video transmission over a wireless link," *IEEE Transactions on Vehicular Technology*, vol. 58, no. 3, pp. 1229–1244, 2009.

[18] "CC2500 Cost Low-Power 2. 4 GHz RF Transceiver, (Rev.C)," Datasheet from TI's website.

[19] B. Razavi, *RF Microelectronics*, Prentice-Hall, Englewood Cliffs, NJ, USA, 1998.

[20] D. C. Daly and A. P. Chandrakasan, "An energy-efficient OOK transceiver for wireless sensor networks," *IEEE Journal of Solid-State Circuits*, vol. 42, no. 5, pp. 1003–1010, 2007.

[21] A. Y. Wang and C. G. Sodini, "On the energy efficiency of wireless transceiver," in *Proceedings of the IEEE International Conference on Communication (ICC '06)*, pp. 3783–3787, 2006.

[22] D. A. Bryan, "QAM for terrestrial and cable transmission," *IEEE Transactions on Consumer Electronics*, vol. 41, no. 3, pp. 383–391, 1995.

[23] K. H. Huang and C. K. Wang, "A cost effective binary FSK demodulator for low-IF radios," in *Proceedings of the International Symposium on VLSI Technology, Systems, and Applications*, pp. 133–136, April 2001.

[24] T. S. Rappaport, *Wireless Communications: Principles and Practice*, Pearson Education Asia Limited and Publishing House of Electronics Industry, 2nd edition, 2004.

[25] G. Hanington, P. F. Chen, P. M. Asbeck, and L. E. Larson, "High-efficiency power amplifier using dynamic power-supply voltage for CDMA applications," *IEEE Transactions on Microwave Theory and Techniques*, vol. 47, no. 8, pp. 1471–1476, 1999.

[26] C. Fan, P. Zhang, B. Xu, and C. Wu, *Principles of Communications*, Publishing House of National Defense Inustry, 5th edition, 2001.

[27] J. Y. Hasani and M. Kamarei, "Analysis and optimum design of a class E RF power amplifier," *IEEE Transactions on Circuits and Systems I*, vol. 55, no. 6, pp. 1759–1768, 2008.